

structure was observed in Phase III. In the present calculation, however, the II-III transition and the long-period structure in Phase III are ignored for simplicity. The calculation only aims to interpret the experimental results qualitatively.

The Helmholtz free energy  $A$  given by Mitsui for a clamped crystal is<sup>4)</sup>

$$A = -\frac{\beta}{2}(P_1^2 + P_2^2) - \beta' P_1 P_2 - \frac{V}{\mu}(P_1 - P_2) + \frac{kTN}{4} \sum_{i=1}^2 \left\{ \left(1 + \frac{2P_i}{N\mu}\right) \ln \left(1 + \frac{2P_i}{N\mu}\right) + \left(1 - \frac{2P_i}{N\mu}\right) \ln \left(1 - \frac{2P_i}{N\mu}\right) - 2 \ln 2 \right\}, \quad (1)$$

$$G = -\frac{\beta}{2}(P_1^2 + P_2^2) - \beta' P_1 P_2 - \frac{V}{\mu}(P_1 - P_2) + \frac{\xi}{4}(P_1^4 + P_2^4) + \frac{\zeta}{2} P_1^2 P_2^2 + \frac{kTN}{4} \sum_{i=1}^2 \left\{ \left(1 + \frac{2P_i}{N\mu}\right) \ln \left(1 + \frac{2P_i}{N\mu}\right) + \left(1 - \frac{2P_i}{N\mu}\right) \ln \left(1 - \frac{2P_i}{N\mu}\right) - 2 \ln 2 \right\}. \quad (2)$$

According to Ishibashi and Takagi<sup>6)</sup> eq. (2) is rewritten by introducing reduced quantities as;

$$g = -\frac{a_1}{2}(x_1^2 + x_2^2) - a_2 x_1 x_2 - (x_1 - x_2) + \frac{a_3}{4}(x_1^4 + x_2^4) + \frac{a_4}{2} x_1^2 x_2^2 + \frac{t}{2} \sum_{i=1}^2 \{ (1 + x_i) \ln(1 + x_i) + (1 - x_i) \ln(1 - x_i) \}, \quad (3)$$

where  $g = 2(G + kTN \ln 2)/(NV)$ ,  $x_1 = 2P_1/(N\mu)$ ,  $x_2 = 2P_2/(N\mu)$ ,  $t = kT/V$ ,  $a_1 = \beta N\mu^2/(2V)$ ,  $a_2 = \beta' N\mu^2/(2V)$ ,  $a_3 = \xi N^3 \mu^4/(8V)$ , and  $a_4 = \zeta N^3 \mu^4/(8V)$ .

The expansion coefficients  $a_i$  are generally dependent both upon reduced temperature  $t$  and upon hydrostatic pressure  $p$  as  $a_i = a_i^{00} + a_i^{10}t + a_i^{01}p + a_i^{11}pt + \dots$ . For simplicity, temperature dependence of  $a_i$  is neglected. The effect of hydrostatic pressure is more significant for the lower-order expansion coefficients. Possible pressure variation of  $a_1$  affects mainly the pressure coefficients of transition points, and it is ignored in the present calculation since the calculation aims to demonstrate the  $p$ - $T$  phase diagram only in a qualitative way. Then, the next lowest expansion coefficient  $a_2$  is assumed to depend linearly upon pressure as

$$a_2 = a_2^{00} + a_2^{01}p. \quad (4)$$

The other coefficients are assumed to be constants.

The spontaneous sublattice polarizations  $x_1^s$ ,  $x_2^s$  are obtained by solving

where  $P_1$  and  $P_2$  are sublattice polarizations,  $\mu$  is the dipole moment of a molecular dipole unit,  $N$  is the number of the dipoles per unit volume. The parameter  $V$  measures the asymmetry of the potential at a dipole site.<sup>4)</sup> As is well known the elastic Gibbs function for a free crystal contains higher order terms of  $P_i$ 's. Third order terms of  $P_i$ 's may be introduced because of existence of  $(P_1 - P_2)$  term in eq. (1). However, in the present calculation the third order terms are neglected; this means that the asymmetry parameter  $V$  is assumed to be independent of lattice strains.\* Then, the resultant elastic Gibbs function  $G$  is expressed to the fourth order terms of  $P_i$ 's as;

$$\frac{\partial g}{\partial x_1} = -a_1 x_1 - a_2 x_2 - 1 + a_3 x_1^3 + a_4 x_1 x_2^2 + t \cdot \tanh^{-1} x_1 = 0, \quad (5)$$

$$\text{and } \frac{\partial g}{\partial x_2} = -a_1 x_2 - a_2 x_1 + 1 + a_3 x_2^3 + a_4 x_1^2 x_2 + t \cdot \tanh^{-1} x_2 = 0, \quad (6)$$

simultaneously. The reduced ferroelectric and antiferroelectric polarizations  $P_F$ ,  $P_A$  are expressed by

$$P_F = (x_1 + x_2)/2, \quad (7)$$

$$\text{and } P_A = (x_1 - x_2)/2, \quad (8)$$

respectively. The reduced dielectric susceptibility  $\chi_F$  is obtained as

$$\chi_F^{-1} = \left( \frac{\partial^2 g}{\partial P_F^2} \right)_{E=0} = \left( \frac{\partial^2 g}{\partial x_1^2} + \frac{\partial^2 g}{\partial x_2^2} + 2 \frac{\partial^2 g}{\partial x_1 \partial x_2} \right)_{E=0} = -2(a_1 + a_2) + 4a_4 x_1^s x_2^s + (3a_3 + a_4) \{ (x_1^s)^2 + (x_2^s)^2 \} + t \{ [1 - (x_1^s)^2]^{-1} + [1 - (x_2^s)^2]^{-1} \}. \quad (9)$$

\* Inclusion of the third order terms did not cause a drastic alternation of the results.

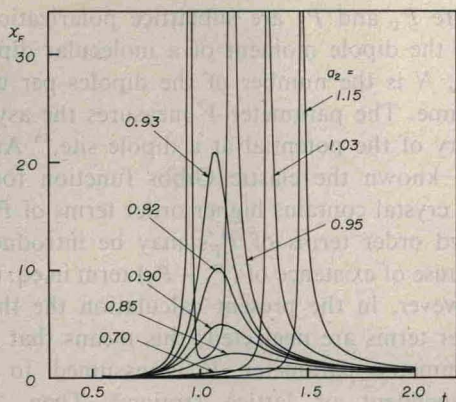


Fig. 8. Calculated reduced temperature  $t$  dependence of the dielectric susceptibility  $\chi_F$  for various values of  $a_2$ .  $a_1=0.45$ ,  $a_3=-0.5$ ,  $a_4=-0.2$ .

Starting from eq. (3) one may calculate using eqs. (5)–(9) the reduced values of dielectric susceptibility  $\chi_F$  and spontaneous ferro- and antiferroelectric polarizations  $P_F^s$ ,  $P_A^s$  as functions of  $t$  and  $a_i$ 's. The calculation was carried out numerically with an electronic computer FACOM 230-75 for various sets of  $a_i$ 's. Figure 8 shows the  $t$ -dependence of  $\chi_F$  for different values of  $a_2$ . Here the other parameters are fixed to be  $a_1=0.45$ ,  $a_3=-0.5$ , and  $a_4=-0.2$ . When  $a_2$  is less than 0.94, no phase transition takes place and the system is antiferroelectric throughout whole range of  $t$ . However, a broad peak of the susceptibility becomes progressively intense and sharp as  $a_2$  increases. In a range  $0.94 < a_2 < 1.0$ , the dielectric susceptibility shows two anomalies, and a ferroelectric phase (denoted as  $F_1$ ) is stabilized between them. When  $a_2$  is larger than 1.0, second ferroelectric phase ( $F_2$ ) is stable in a lower  $t$  region. As  $a_2$  further increases the lower temperature peak of  $\chi_F$  is masked by the direct transition between two ferroelectric phases. Since the parameter  $a_2$  is assumed to be a linear function of pressure, Fig. 8 represents the temperature dependence of the susceptibility at various pressures corresponding to Figs. 1 and 2 for  $(\text{NH}_4)_3\text{H}(\text{SO}_4)_2$ . Figure 9 shows the  $a_2$  dependence of the inverse of the maximum susceptibility  $1/\chi_F^{\text{max}}$  in a region of  $a_2 < 0.94$  where ferroelectric phases are not stabilized. The inverse of the maximum susceptibility linearly decreases with increasing  $a_2$  and tends to zero at  $a_2=0.94$ . Figure 9 qualitatively represents the observed behavior of  $1/\epsilon_{\text{max}}$  vs

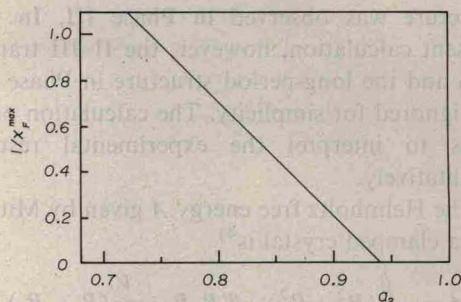


Fig. 9. Variation of the inverse of the maximum susceptibility  $1/\chi_F^{\text{max}}$  with  $a_2$ .  $a_1=0.45$ ,  $a_3=-0.5$ ,  $a_4=-0.2$ .

$p$  of  $(\text{NH}_4)_3\text{H}(\text{SO}_4)_2$  shown in Fig. 5. Figures 10 and 11 show  $t$ -dependence of the spontaneous ferro- and antiferroelectric polarizations  $P_F^s$  and  $P_A^s$  for different values of  $a_2$ , respectively.

In the limit of the present approximation the transition between two ferroelectric states  $F_1$  and  $F_2$  is isomorphous one;<sup>8)</sup> namely the symmetry of the crystal does not change during

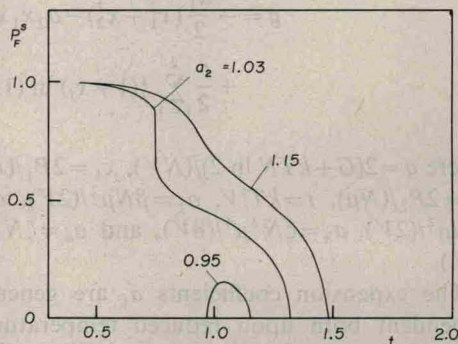


Fig. 10. Reduced temperature  $t$  dependence of the spontaneous ferroelectric polarization  $P_F^s$  for different  $a_2$ .  $a_1=0.45$ ,  $a_3=-0.5$ ,  $a_4=-0.2$ .

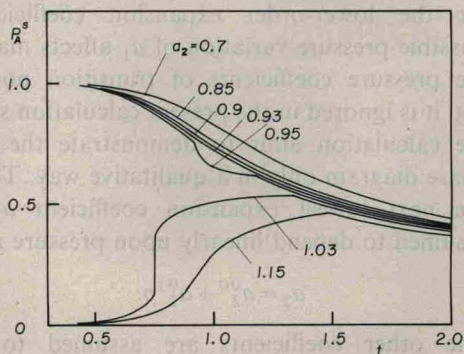


Fig. 11. Reduced temperature  $t$  dependence of the spontaneous antiferroelectric polarization  $P_A^s$  for different  $a_2$ .  $a_1=0.45$ ,  $a_3=-0.5$ ,  $a_4=-0.2$ .